$[Ru(bpy)_3]^{2+}$ to variations in solvent. Except for some sharpening, the emission is nearly unaffected. This emission sharpening can probably be attributed to the increased rigidity of the environment similar to the sharpening observed when the complex is measured in a rigid glass at 77 K.

The shortening of the lifetime in PVA with increasing concentration can probably be attributed to concentration quenching. On the basis of an assumed density of the matrix equal to that of bulk PVA, we can calculate a Stern-Volmer self-quenching constant, K_{SV}, from eq 3, where τ_0 is the un-

$$K_{SV} = [(\tau_0/\tau) - 1]/[[Ru(bpy)_3]^{2+}] \quad (3)$$

quenched lifetime (taken as the value in the most dilute matrix) and τ is the quenched lifetime. For the quantum counter sample in PVA, we obtain $K_{SV} = 0.4\ M^{-1}$. The onset of nonexponentiality in the decay curves at high concentrations can probably be attributed to one of two sources. As the concentration rises, the complex molecules may be crowded together into adjacent occupancy sites in the polymer, giving rise to an increase in nearest-neighbor quenching. Alternatively, we may just be observing the onset of crystallization in microscopic domains. This latter possibility seems most probable for the following reasons. The nonexponentiality becomes most severe after the visual appearance of crystals and the lifetime of the fast component are the same for the crystallized sample and the quantum counter where no discernible crystallization is apparent.

We suggest that the somewhat poorer spectral flatness of the PVP film may be correlated with the much lower solubility of $[Ru(bpy)_3]^{2+}$ in this matrix. Even at the low but near saturated concentration used in the PVP counter, we may still be observing the presence of some microdomain crystallization.

Acknowledgment. We gratefully acknowledge support by the Air Force Office of Scientific Research (Chemistry) (Grant AFOSR 78-3590) and the donors of the Petroleum Research Fund, administered by the American Chemical Society. We also acknowledge the use of the University of Virginia laser facility, which was purchased in part from NSF Grant CHE 77-09296. We also thank GAF Corp. for the gift of the PVP polymer.

Registry No. $[Ru(bpy)_3]Cl_2$, 14323-06-9; PVA, 9002-89-5; PVP, 9003-43-4.

Contribution from the Departments of Chemistry, The Pennsylvania State University, University Park, Pennsylvania 16802, and Northern Illinois University, DeKalb, Illinois 60115

Metal-to-Ligand Charge-Transfer Spectra of Some *cis*- and *trans*-$[Pt(PEt_3)_2(X)(Y)]$ Complexes

DAVID A. ROBERTS,[1a] W. ROY MASON,[1b] and GREGORY L. GEOFFROY*[1a]

Received June 18, 1980

Solution electronic absorption and magnetic circular dichroism (MCD) spectral data at 298 K are reported for *cis*-$[Pt(PEt_3)_2X_2]$, *cis*-$[Pt(PEt_3)_2(Me)X]$ (X = Cl, Br), *cis*-$[Pt(PEt_3)_2(R)_2]$ (R = Me, Et), *trans*-$[Pt(PEt_3)_2X_2]$ (X = Cl, Br, I), *trans*-$[Pt(PEt_3)_2(H)X]$, *trans*-$[Pt(PEt_3)_2(Me)X]$, and *trans*-$[Pt(PEt_3)_2(Et)X]$ (X = Cl, Br). Electronic absorption spectra obtained at 77 K in glassy solution (7/4 methylcyclohexane/pentane) are also reported for *cis*-$[Pt(PEt_3)_2Me_2]$, *cis*-$[Pt(PEt_3)_2(Me)Cl]$, *trans*-$[Pt(PEt_3)_2(R)Cl]$ (R = Me, Et), and *trans*-$[Pt(PEt_3)_2Br_2]$. All of these complexes exhibit intense absorptions in the UV spectral region which are assigned as metal-to-ligand charge transfer (MLCT) transitions from occupied Pt 5d orbitals to empty phosphorus 3d orbitals of the PEt_3 ligands. Some of the halide complexes also exhibit ligand field (LF) and ligand-to-metal charge-transfer (LMCT) bands in addition to the MLCT transitions. Detailed spectral assignments are given, and the relative energies of the MLCT transitions as a function of the X and Y ligands are discussed. For the cis complexes, the ordering $Et_2 < Me_2 < MeX < X_2$ (X = Cl, Br) is found whereas for the trans complexes the ordering $HX < EtX < MeX < X_2$ (X = Cl, Br) obtains. Since the positioning of the MLCT transitions is a sensitive function of the Pt oxidation state, the above orderings imply that the metal ion becomes less oxidized upon descending the series X > Me > Et > H.

Introduction

Square-planar complexes of metals with the d^8 electronic configuration which possess π-acceptor ligands generally show intense metal-to-ligand charge-transfer (MLCT) bands in their electronic absorption spectra.[2-8] These result from electronic excitation from occupied MO's, mainly of metal *n*d character, to empty ligand-based orbitals. Excitation of this type may be viewed as an incipient oxidation of the metal ion and the energetics of excitation reflect metal orbital stability and are related to the redox properties of the metal ion in the complex. Thus the MLCT excited states, which are often the lowest energy-allowed excited states, are of considerable interest not only from the standpoint of electronic structure but also in formulating electronic models for reaction pathways involving metal oxidation.

Hydride and alkyl ligands play a pivotal role in organometallic chemistry and are invoked as key intermediates in numerous transition metal catalyzed or mediated organic reactions. Yet, surprisingly few studies have been conducted which have examined the electronic structures of complexes of these ligands, and no single comparative study is available for a series of complexes in which these and accompanying ligands are systematically varied. In order to partly fill this void, we have measured the electronic absorption and magnetic circular dichroism (MCD) spectra of a series of planar *cis*- and *trans*-$[Pt(PEt_3)_2(X)(Y)]$ complexes in which X and Y include hydride, alkyl, and halide ligands. This data has allowed us to assess the relative oxidation state of the metal ion in these complexes and to correlate the oxidation state with

(1) (a) The Pennsylvania State University. (b) Northern Illinois University.
(2) Geoffroy, G. L.; Isci, H.; Litrenti, J.; Mason, W. R. *Inorg. Chem.* **1977**, *16*, 1950.
(3) Epstein, R. A.; Geoffroy, G. L.; Keeney, M. E.; Mason, W. R. *Inorg. Chem.* **1979**, *18*, 478.
(4) Isci, H.; Mason, W. R. *Inorg. Chem.* **1975**, *14*, 905.
(5) Isci, H.; Mason, W. R. *Inorg. Chem.* **1975**, *14*, 913.
(6) Geoffroy, G. L.; Wrighton, M. S.; Hammond, G. S.; Gray, H. B. *J. Am. Chem. Soc.* **1974**, *96*, 3105.
(7) Brady, R.; Flynn, B. R.; Geoffroy, G. L.; Gray, H. B.; Peone, J., Jr.; Vaska, L. *Inorg. Chem.* **1976**, *15*, 1485.
(8) Mason, W. R.; Gray, H. B. *J. Am. Chem. Soc.* **1968**, *90*, 5721.

0020-1669/81/1320-0789$01.00/0

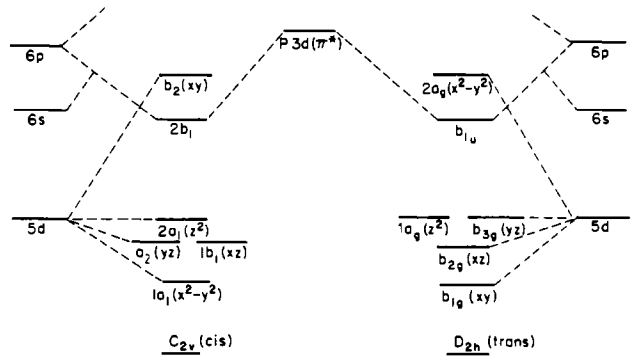

Figure 1. One-electron molecular orbital energy level diagrams for planar complexes of C_{2v} and D_{2h} symmetries.

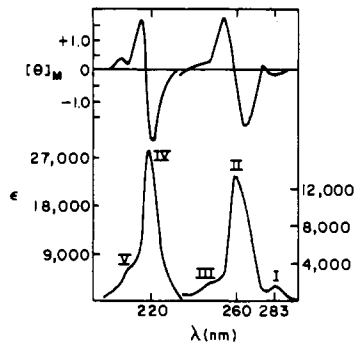

Figure 2. Electronic absorption (lower curve) and MCD (upper curve) spectra of $[(n\text{-}C_4H_9)_4N]_2[Pt(CN)_4]$ in CH_3CN solution. Reproduced with permission from ref 4.

the σ-donor properties of the ligands.

Experimental Section

The complexes *trans*-$[Pt(PEt_3)_2X_2]$ (X = Cl, Br, I),[9] *trans*-$[Pt(PEt_3)_2(H)X]$ (X = Cl, Br),[10] *trans*-$[Pt(PEt_3)_2(Me)X]$ (X = Cl, Br),[11] *trans*-$[Pt(PEt_3)_2(Et)X]$ (X = Cl, Br),[12] *cis*-$[Pt(PEt_3)_2X_2]$ (X = Cl, Br),[9] *cis*-$[Pt(PEt_3)_2(Me)X]$ (X = Cl, Br),[11] *cis*-$[Pt(PEt_3)_2Me_2]$,[11] and *cis*-$[Pt(PEt_3)_2Et_2]$[12] were prepared by published procedures. The purity of the complexes was ascertained by their ^{31}P NMR and mass spectra and comparison of their IR spectra and melting points to reported values. Electronic absorption spectra were obtained on a Cary 17 or Cary 1501 spectrophotometer using 1.0-cm path length quartz cells. The MCD spectra were recorded on a Jasco ORD/UV-5 spectrometer equipped with a CD attachment, using a permanent magnet with a field of 1.0 T. Spectra at 77 K were measured in frozen 7/4 methylcyclohexane/pentane solutions with use of a quartz Dewar with optically flat Suprasil quartz windows. The 77 K spectra were corrected for 20% solvent contraction upon cooling.

Methylcyclohexane (Baker analyzed reagent grade) and pentane (Aldrich Chemical Co. spectrophotometric grade) were dried over calcium hydride and then passed through an alumina/$AgNO_3$ column to remove aromatic impurities.[13] Acetonitrile (spectrophotometric grade) was obtained from Aldrich Chemical Co. or MCB Reagents and was used without further purification.

Results

Molecular Orbital Energy Levels and Excited States. In the following discussion the *cis*- and *trans*-$[Pt(PEt_3)_2(X)(Y)]$ complexes are assumed to approximate C_{2v} and D_{2h} symmetries, respectively, when X = Y. The one-electron molecular orbital energy level diagrams which are appropriate for these symmetries are shown in Figure 1. In both cases the z axis is taken perpendicular to the molecular plane. The C_2 symmetry axis of the cis complex and the two PEt_3 ligands of the trans complex lie along the x axis. The diagrams shown in Figure 1 must be modified when X $\neq$ Y, but the spectral data discussed below indicates that in general these modifications are small.

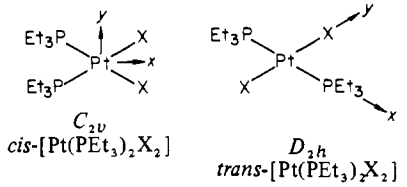

The ground states of all the Pt(II) complexes examined in this work are diamagnetic and totally symmetric. The MLCT excited configurations are produced by excitation of electrons from the occupied Pt 5d orbitals to the primarily ligand-based $2b_1$ (C_{2v}) or b_{1u} (D_{2h}) orbitals which are mainly phosphorus 3d but with some admixture of the $6p_z$ orbitals. Because of the strong Pt spin–orbit coupling ($\zeta_{5d} \approx 0.30$–$0.35\ \mu m^{-1}$), the singlet and triplet MLCT states become mixed, and considerable intensities can be observed for formally spin-forbidden transitions.

The MLCT states expected for the *cis*- and *trans*-$[Pt(PEt_3)_2X_2]$ complexes are analogous to those described for the higher symmetry D_{4h} complexes studied earlier.[2,4,5] These states result from the three dipole-allowed one-electron excitations $d_{z^2} \rightarrow \pi^*$, $d_{xz} \rightarrow \pi^*$, and $d_{yz} \rightarrow \pi^*$ in which π^* is a general representation for the ligand-based orbital described above. In the *cis*-$[Pt(PEt_3)_2(X)(Y)]$ complexes of C_s symmetry, the $d_{x^2-y^2} \rightarrow \pi^*$ excitation, which is orbitally forbidden in higher symmetry also becomes formally allowed. Even though the singlet and triplet MLCT states are intermixed by Pt spin–orbit coupling, it is still useful to refer to transitions to these states from the singlet ground state in terms of their predominant spin components. For example, the notation $^1[d_{z^2} \rightarrow \pi^*]$ and $^3[d_{z^2} \rightarrow \pi^*]$ refer to d_{z^2} excitation to MLCT states of singlet and triplet parentage, respectively. This notation is used in Table I to indicate the specific spectral assignments.

The MCD spectra for the *cis*- and *trans*-$[Pt(PEt_3)_2(X)(Y)]$ complexes should exhibit only B terms because the low symmetries of the complexes remove all strict degeneracies. However, if two MLCT transitions which have B terms of opposite sign lie sufficiently close in energy (less than their bandwidths), the MCD spectrum will give the appearance of an A term, characteristic of transitions to true degenerate states. Such a situation has been observed in several cases for MLCT spectra in planar complexes, even in higher symmetry complexes where true degeneracies do exist,[2-4,14] and has been called a pseudo-A term.[14] The signs, if not the relative magnitudes of the B terms and also the pseudo-A terms, can be predicted from eq 1,[2,14] where β is the Bohr magneton, ΔW_{kj}

$$B(a \rightarrow j) = \frac{i\beta}{\Delta W_{kj}} \sum_{k \neq j} \langle j|\mathbf{l} + 2\mathbf{s}|k\rangle \cdot \langle a|\mathbf{m}|j\rangle \mathbf{x} \langle k|\mathbf{m}|a\rangle \qquad (1)$$

is the energy difference between states k and j, and the matrix elements are of orbital (**l**) and spin (**s**) angular momentum and the dipole operator (**m**). The states j and k are approximated by one-electron atomic orbital functions, and the summation is limited to the states k closest in energy to j because of the ΔW_{kj}^{-1} term. This approximate approach has provided predictions that compare favorably with experiments for the MLCT spectra of several higher symmetry complexes.[2]

Electronic Absorption and MCD Spectra. Specific spectral assignments for the complexes studied in this work are given in Table I, and the rationale for these assignments is detailed

(9) Jenkins, K. A. *Z. Anorg. Allg. Chem.* **1936**, *229*, 225.
(10) Chatt, J.; Shaw, B. L. *J. Chem. Soc.* **1962**, 5075.
(11) Chatt, J.; Shaw, B. L. *J. Chem. Soc.* **1959**, 705.
(12) Chatt, J.; Shaw, B. L. *J. Chem. Soc.* **1959**, 4020.
(13) Murray, E. C.; Keller, R. N. *J. Org. Chem.* **1969**, *34*, 2234.
(14) Piepho, S. B.; Schatz, P. N.; McCaffery, A. J. *J. Am. Chem. Soc.* **1969**, *91*, 5994.

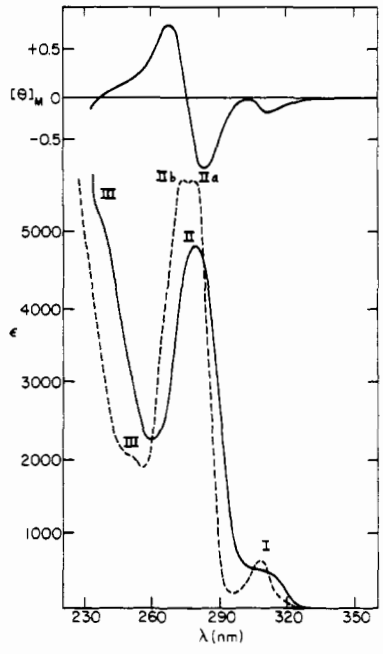

Figure 3. Electronic absorption (lower curves) and MCD (upper curve) spectra of *cis*-[Pt(PEt$_3$)$_2$(Me)$_2$]: (—) 298 K, CH$_3$CN solution; (---) 77 K, 7/4 methylcyclohexane/pentane glassy solution.

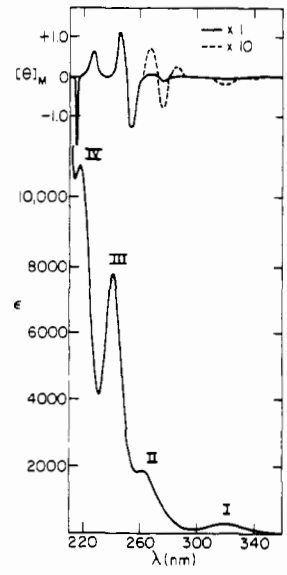

Figure 4. Electronic absorption (lower curve) and MCD (upper curve) spectra of *cis*-[Pt(PEt$_3$)$_2$Cl$_2$] in CH$_3$CN solution.

below. The best studied example of a Pt(II) complex with π-accepting ligands which shows MLCT bands is [Pt(CN)$_4$]$^{2-}$.[4,14] For comparison with the results reported herein, the spectra and corresponding assignments of this complex are briefly reviewed.

[Pt(CN)$_4$]$^{2-}$. The electronic absorption and MCD spectra of [(*n*-C$_4$H$_9$)$_4$N]$_2$[Pt(CN)$_4$] in acetonitrile solution have been given in ref 4 and are reproduced in Figure 2. The specific band assignments which have been derived, with the notation employed herein and the labels of Figure 2, are as follows: band I, 3.54 μm^{-1}, ^{3}[$d_{z^2} \rightarrow \pi^*$]; band II, 3.85 μm^{-1}, {^{1}[$d_{z^2} \rightarrow \pi^*$], ^{3}[$d_{xy}$, $d_{yz} \rightarrow \pi^*$]}; band IV, 4.55 μm^{-1}, ^{1}[d_{xz}, $d_{yz} \rightarrow \pi^*$]. Bands III and V at 4.05 and 4.70 μm^{-1} were assigned to excited-state vibrations associated with the ^{1,3}[d_{xz}, $d_{yz} \rightarrow \pi^*$] states. Similar spectra were obtained and analogous assignments derived for the [Pt(CN)$_2$en] and *trans*-[Pt(CN)$_2$(NH$_3$)$_2$] complexes which are symmetry related to the *cis*- and *trans*-[Pt(PEt$_3$)$_2$(X)(Y)] complexes studied herein.[4]

***cis*-[Pt(PEt$_3$)$_2$(R)$_2$] (R = Me, Et).** The band patterns observed in the MCD and electronic absorption spectra of *cis*-[Pt(PEt$_3$)$_2$Me$_2$] (Figure 3) are remarkably similar to those found for [Pt(CN)$_4$]$^{2-}$[4,14] (Figure 2), and similar spectra assignments are thus indicated. Since the methyl ligands are not involved in π bonding, the MLCT states of *cis*-[Pt(PEt$_3$)$_2$Me$_2$] should in fact closely parallel those of [Pt(CN)$_4$]$^{2-}$, with the lowest energy states being expected from $d_{z^2} \rightarrow \pi^*$ followed by states from $d_{xz} \rightarrow \pi^*$ and $d_{yz} \rightarrow \pi^*$ excitation at higher energy. The lowest energy band I at 3.28 μm^{-1} exhibits a positive *B* term (negative ellipticity) in the MCD spectrum, while the higher energy bands at 3.64 μm^{-1} (II) and 4.86 μm^{-1} (IV) exhibit pseudo-*A* terms indicating two or more overlapping transitions. The lowest energy band is assigned as ^{3}[$d_{z^2} \rightarrow \pi^*$], the lowest energy component of which is predicted from eq 1 to have a positive *B* term. Band II is assigned to the overlapping transitions ^{1}[$d_{z^2} \rightarrow \pi^*$], ^{3}[$d_{xz} \rightarrow \pi^*$], and ^{3}[$d_{yz} \rightarrow \pi^*$] which give rise to the pseudo-*A* term in the MCD spectrum. The positive pseudo-*A* term observed in the MCD spectrum indicates that the ^{1}[$d_{z^2} \rightarrow \pi^*$] MLCT transition is lowest in energy since, of the three transitions, only it yields a positive *B* term. Note that partial resolution of these transitions is achieved when the spectrum is recorded at 77 K in a glassy solution (Figure 3). Thus band IIa at 3.61 μm^{-1} in the 77 K spectrum is attributed to the ^{1}[$d_{z^2} \rightarrow \pi^*$] transition and band IIb at 3.66 μm^{-1} to the ^{3}[$d_{xz} \rightarrow \pi^*$], ^{3}[$d_{yz} \rightarrow \pi^*$] transitions.

Band IV is attributed to the nearly degenerate overlapping transitions ^{1}[$d_{xz} \rightarrow \pi^*$] and ^{1}[$d_{yz} \rightarrow \pi^*$]. The positive pseudo-*A* term is analogous to the positive *A* term observed for the degenerate ^{1}[d_{xz}, $d_{yz} \rightarrow \pi^*$] transition for [Pt(CN)$_4$]$^{2-}$.[4,14] Finally, band III which appears as a shoulder in the absorption spectrum, is assigned as ^{3}[$d_{x^2-y^2} \rightarrow \pi^*$]. This transition should be slightly higher in energy than the ^{3}[$d_{xz} \rightarrow \pi^*$], ^{3}[$d_{yz} \rightarrow \pi^*$] transitions due to the greater degree of π bonding possible between the two PEt$_3$ ligands and the in-plane $d_{x^2-y^2}$ orbital compared to the out-of-plane d_{xz}, d_{yz} orbitals.

Although not as well resolved, the electronic absorption spectrum of *cis*-[Pt(PEt$_3$)$_2$Et$_2$] is similar to that of the dimethyl analogue, and analogous assignments are suggested (Table I). One notable feature is the shift to lower energy in the ^{1,3}[$d_{z^2} \rightarrow \pi^*$] transitions for the Et$_2$ complex when compared to *cis*-[Pt(PEt$_3$)$_2$Me$_2$], although the energetics of the ^{3}[d_{xz}, $d_{yz} \rightarrow \pi^*$] transitions are comparable.

***cis*-[Pt(PEt$_3$)$_2$X$_2$] (X = Cl, Br).** The MCD and absorption spectra of *cis*-[Pt(PEt$_3$)$_2$Cl$_2$] (Figure 4) and *cis*-[Pt(PEt$_3$)$_2$Br$_2$] are somewhat more complicated than those of the dimethyl complex due to the appearance of ligand field (LF) and ligand-to-metal charge-transfer (LMCT) transitions, the latter from halide-based orbitals to the empty b_2 (d_{xy}) orbital. The weak band at 3.13 μm^{-1} (I) and the broad MCD *B* terms at 3.18 and 3.62 μm^{-1} for *cis*-[Pt(PEt$_3$)$_2$Cl$_2$] are attributed to LF transitions. A similar assignment is appropriate for the band at 2.95 μm^{-1} (I) and the MCD features at 2.74 and 2.94 μm^{-1} in the spectra of *cis*-[Pt(PEt$_3$)$_2$Br$_2$]. These bands have no counterpart in the dimethyl complex, presumably because the high position of CH$_3$ in the spectrochemical series places corresponding transitions at high energy beneath the more intense MLCT bands. Support for the assignment of these bands as LF transitions comes from the energy difference between the corresponding bands (I) in the chloro and bromo complexes (0.18 μm^{-1}) which is in the same direction and of the same magnitude as the energy difference between the lowest singlet LF transitions in [PtCl$_4$]$^{2-}$[8] and [PtBr$_4$]$^{2-}$[15] (0.16 μm^{-1}).

(15) Kroening, R. F.; Rush, R. M.; Martin, D. S., Jr.; Clardy, J. C. *Inorg. Chem.* **1974**, *13*, 1366.

Table I. Electronic Absorption and Magnetic Circular Dichroism Spectral Data[a]

complex	band	abs λ_{max}, nm	abs $\bar{\nu}_{max}$, μm^{-1}	abs ϵ_{max}, M^{-1} cm^{-1}	MCD[b] $\bar{\nu}$, μm^{-1} ($[\theta]_m$)	assignt
$[(n\text{-}C_4H_9)_4N]_2[Pt(CN)_4]$[c] (298 K)	I	283	3.54	1230		$^3[d_{z^2} \rightarrow \pi^*]$
	II	260	3.845	12900		$^1[d_{z^2} \rightarrow \pi^*]$, $^3[d_{x^2}, d_{yz} \rightarrow \pi^*]$
	III	247 sh	4.05 sh	1840		II + ν_{CN}
	IV	220	4.55	29300		$^1[d_{xz}, d_{yz} \rightarrow \pi^*]$
	V	213 sh	4.70 sh	8780		IV + ν_{CN}
cis-$[Pt(PEt_3)_2Me_2]$ (298 K)	I	305 sh	3.28 sh	510	3.21 (−0.154)	$^3[d_{z^2} \rightarrow \pi^*]$
	II	275	3.64	4800	3.55 (−0.78) 3.66 (0) 3.76 (+0.57)	$^1[d_{z^2} \rightarrow \pi^*]$, $^3[d_{xz}, d_{yz} \rightarrow \pi^*]$
	III	235 sh	4.25 sh	5660		$^3[d_{x^2-y^2} \rightarrow \pi^*]$
	IV	206	4.86	23000	4.50 (−1.9) 4.63 (0) 4.73 (+1.2)	$^1[d_{xz}, d_{yz} \rightarrow \pi^*]$
cis-$[Pt(PEt_3)_2Me_2]$[d] (77 K)	I	306	3.26	622		$^3[d_{z^2} \rightarrow \pi^*]$
	IIa	277	3.61	5640		$^1[d_{z^2} \rightarrow \pi^*]$
	IIb	273	3.66	5640		$^3[d_{xz}, d_{yz} \rightarrow \pi^*]$
	III	247	4.06	2870		$^3[d_{x^2-y^2} \rightarrow \pi^*]$
cis-$[Pt(PEt_3)_2Et_2]$ (298 K)	I	323 sh	3.10	400		$^3[d_{z^2} \rightarrow \pi^*]$
	IIa	293 sh	3.40	2060		$^1[d_{z^2} \rightarrow \pi^*]$
	IIb	275 sh	3.64	2670		$^3[d_{xz}, d_{yz} \rightarrow \pi^*]$
	III	245 sh	4.08	3870		$^3[d_{x^2-y^2} \rightarrow \pi^*]$
	IV	203 sh	4.93	24000		$^1[d_{xy}, d_{yz} \rightarrow \pi^*]$
cis-$[Pt(PEt_3)_2Cl_2]$ (298 K)	I	319	3.13	370	3.18 (−0.02)	LF
					3.62 (+0.024)	LF
	II	262	3.81	1960	3.73 (−0.079) 3.79 (0.0) 3.86 (+0.074)	$^3[d_{z^2} \rightarrow \pi^*]$
	III	242	4.14	7400	4.08 (−1.27) 4.16 (0.0) 4.24 (+1.11)	$^1[d_{z^2} \rightarrow \pi^*]$, $^3[d_{xz}, d_{yz} \rightarrow \pi^*]$
	IV	219	4.56	10900	4.60 (+0.63)	π-LMCT
	V	202	4.96	41500	4.81 (−3.3) 4.90 (0.0)	$^1[d_{xz}, d_{yz} \rightarrow \pi^*]$ σ-LMCT
cis-$[Pt(PEt_3)_2Br_2]$ (298 K)	I	339	2.95 sh	450	274 (−0.015)	LF
					294 (0.0)	LF
	II	297	3.37	1660	3.47 br (+0.072)	π-LMCT
	III	264	3.78 sh	1620	3.72 (−0.093)	$^3[d_{z^2} \rightarrow \pi^*]$
	IV	247	4.05 sh	6900	3.98 (−0.96) 4.10 (0.0) 4.22 (+0.66)	$^1[d_{z^2} \rightarrow \pi^*]$, $^3[d_{xz}, d_{yz} \rightarrow \pi^*]$
	V	227	4.4 sh	16200	4.69 (−3.6) 4.81 (0.0)	σ-LMCT, $^1[d_{xz}, d_{yz} \rightarrow \pi^*]$
	VI	208	4.81	44900		
cis-$[Pt(PEt_3)_2(Me)Cl]$ (298 K)	I	286	3.50 sh	1270	3.45 (−0.12)	$^3[d_{z^2} \rightarrow \pi^*]$
	II	244	4.09	7500	3.89 (−0.75) 4.00 (0.0) 4.13 (+0.72)	$^1[d_{z^2} \rightarrow \pi^*]$, $^3[d_{xz}, d_{yz} \rightarrow \pi^*]$
	III	222	4.5 sh	8900	4.46 sh (−0.13)	$^3[d_{x^2-y^2} \rightarrow \pi^*]$
	IV	207	4.82	16500	4.72 (−1.5) 4.81 (0.0) 4.93 (+1.1)	$^1[d_{xz}, d_{yz} \rightarrow \pi^*]$
cis-$[Pt(PEt_3)_2(Me)Cl]$[d] (77 K)	I	280	3.57	1400		$^3[d_{z^2} \rightarrow \pi^*]$
	IIa	248	4.03	8400		$^1[d_{z^2} \rightarrow \pi^*]$, $^3[d_{xz}, d_{yz} \rightarrow \pi^*]$
	IIb	238	4.20	10500		
cis-$[Pt(PEt_3)_2(Me)Br]$ (298 K)	I	284	3.52 sh	1380	3.44 (−0.11)	$^3[d_{z^2} \rightarrow \pi^*]$
	II	250	4.00	6900	3.86 (−0.86) 3.95 (0) 4.05 (+0.65)	$^1[d_{x^2} \rightarrow \pi^*]$, $^3[d_{xz}, d_{yz} \rightarrow \pi^*]$
	III	220	4.55 sh	15300	4.65 (−1.4)	$^3[d_{x^2-y^2} \rightarrow \pi^*]$
	IV	206	4.85 sh	27500		$^1[d_{xz}, d_{yz} \rightarrow \pi^*]$
	V	201	4.97	29700		LMCT
trans-$[Pt(PEt_3)_2(H)Cl]$ (298 K)	I	302	3.31 sh	910	3.24 (−0.19)	$^3[d_{z^2} \rightarrow \pi^*]$
					3.52 (−0.21)	$^3[d_{yz} \rightarrow \pi^*]$
	II	264	3.78 sh	4600	3.80 (−0.33)	$^1[d_{z^2} \rightarrow \pi^*]$
	III	252	3.96	6050	4.02 (+0.59)	$^1[d_{yz} \rightarrow \pi^*]$
					4.48 (−0.91)	$^3[d_{xz} \rightarrow \pi^*]$
	IV	215	4.65 sh	11000	4.63 (0.00)	$^1[d_{xz} \rightarrow \pi^*]$
	V	196	5.1	21000		π-LMCT/d → p
trans-$[Pt(PEt_3)_2(Me)Cl]$ (298 K)	I	292	3.42 sh	1060	3.32 (−0.20)	$^3[d_{z^2} \rightarrow \pi^*]$
	II	274	3.65 sh	2440	3.61 (−0.21)	$^3[d_{yz} \rightarrow \pi^*]$
	III	254	3.94	5300	3.82 (−0.35) 3.91 (0.0) 4.03 (+0.47)	$^1[d_{z^2} \rightarrow \pi^*]$, $^1[d_{yz} \rightarrow \pi^*]$
					4.37 (−0.23)	$^3[d_{xz} \rightarrow \pi^*]$
	IV	197	5.08	31800		π-LMCT/d → p
trans-$[Pt(PEt_3)_2(Me)Cl]$[d] (77 K)	I	293	3.41	1040		$^3[d_{z^2} \rightarrow \pi^*]$
	II	269	3.72	2500		$^3[d_{yz} \rightarrow \pi^*]$
	III	253	3.95	5800		$^1[d_{z^2} \rightarrow \pi^*]$, $^1[d_{yz} \rightarrow \pi^*]$

Table I (*Continued*)

complex	band	abs λ_{max}, nm	abs $\bar{\nu}_{max}$, μm^{-1}	abs ϵ_{max}, M^{-1} cm^{-1}	MCD[b] $\bar{\nu}$, μm^{-1} ($[\theta]_m$)	assignt
trans-[Pt(PEt$_3$)$_2$(Et)Cl]	I	297	3.37 sh	1130	3.26 (−0.20)	$^3[d_{z^2} \rightarrow \pi^*]$
(298 K)	II	274	3.65 sh	3000	3.55 (−0.18)	$^3[d_{yz} \rightarrow \pi^*]$
	III	258	3.88	5330	3.77 (−0.31), 3.86 (0), 3.98 (+0.45)	$^1[d_{z^2} \rightarrow \pi^*]$, $^1[d_{yz} \rightarrow \pi^*]$
	IV	195	5.13	33200		π-LMCT/d → p
trans-[Pt(PEt$_3$)$_2$(Et)Cl][d]	I	297	3.37	1200		$^3[d_{z^2} \rightarrow \pi^*]$
(77 K)	II	284	3.52	1500		$^3[d_{yz} \rightarrow \pi^*]$
	III	255	3.92	7000		$^1[d_{z^2} \rightarrow \pi^*]$
trans-[Pt(PEt$_3$)$_2$(H)Br]	I	302	3.31 sh	1040	3.22 (−0.19)	$^3[d_{z^2} \rightarrow \pi^*]$
(298 K)					3.47 (−0.19)	$^3[d_{yz} \rightarrow \pi^*]$
	II	258	3.88	5860	3.70 (−0.35), 3.83 (0.0), 3.97 (+0.59)	$^1[d_{z^2} \rightarrow \pi^*]$, $^1[d_{yz} \rightarrow \pi^*]$
					4.48 (−0.76)	$^3[d_{xz} \rightarrow \pi^*]$
	III	215	4.65 sh	14100	4.69 (0.0)	$^1[d_{xz} \rightarrow \pi^*]$
	IV	197	5.07 sh	28000		π-LMCT/d → p
trans-[Pt(PEt$_3$)$_2$(Me)Br]	I	292	3.43 sh	1180	3.33 (−0.18)	$^3[d_{z^2} \rightarrow \pi^*]$
(298 K)	II	274	3.65 sh	2280	3.58 (−0.19)	$^3[d_{yz} \rightarrow \pi^*]$
	III	255	3.92	5300	3.77 (−0.40), 3.89 (0.0), 4.02 (+0.46)	$^1[d_{z^2} \rightarrow \pi^*]$, $^1[d_{yz} \rightarrow \pi^*]$
					4.35 (−0.24)	$^3[d_{xz} \rightarrow \pi^*]$
	IV	217	4.60 sh	17100		$^1[d_{xz} \rightarrow \pi^*]$
	V	198	5.06	48100		π-LMCT/d → p
trans-[Pt(PEt$_3$)$_2$(Et)Br]	I	298	3.36 sh	1270	3.27 (−0.19)	$^3[d_{z^2} \rightarrow \pi^*]$
(298 K)	II	275	3.63 sh	2800	3.57 (−0.17)	$^3[d_{yz} \rightarrow \pi^*]$
					3.73 (−0.37)	$^1[d_{z^2} \rightarrow \pi^*]$
	III	259	3.86	5340	3.83 (0)	$^1[d_{yz} \rightarrow \pi^*]$
					3.97 (+0.49)	$^3[d_{xz} \rightarrow \pi^*]$
	IV	215	4.65 sh	18300	4.48 (−0.54)	$^1[d_{xz} \rightarrow \pi^*]$
	V	198	5.05	37900		π-LMCT/d → p
trans-[Pt(PEt$_3$)$_2$Cl$_2$]	I	305	3.28 sh	640	3.50 (+0.04)	LF
(298 K)	II	267	3.74	10700	3.65 (−0.15)	$^3[d_{yz} \rightarrow \pi^*]$
					3.82 (−0.17)	$^1[d_{z^2} \rightarrow \pi^*]$
	III	248	4.03	11300	4.18 (+0.34)	$^1[d_{yz} \rightarrow \pi^*]$
	IV	221	4.53	4800	4.46 (−0.17)	$^3[d_{xz} \rightarrow \pi^*]$
					4.76 (−0.39)	$^1[d_{xz} \rightarrow \pi^*]$
	V	193	5.17 sh	33300		π-LMCT
trans-[Pt(PEt$_3$)$_2$Cl$_2$][d]	I	303	3.30 sh	510		LF
(298 K)	IIa	270	3.70 sh	6440		$^3[d_{yz} \rightarrow \pi^*]$
	IIb	263	3.80	7820		$^1[d_{z^2} \rightarrow \pi^*]$
	III	249	4.02	13900		$^1[d_{yz} \rightarrow \pi^*]$
	IVa	233	4.29	4590		$^3[d_{xz} \rightarrow \pi^*]$
	IVb	221 sh	4.52	9350		$^1[d_{xz} \rightarrow \pi^*]$
trans-[Pt(PEt$_3$)$_2$Cl$_2$][d]	I	303	3.30	400		LF
(77 K)	IIa	272	3.68 sh	5300		$^3[d_{yz} \rightarrow \pi^*]$
	IIb	260	3.85	7860		$^1[d_{yz} \rightarrow \pi^*]$
	III	248	4.03	17000		$^1[d_{yz} \rightarrow \pi^*]$
	IVa	230	4.35			$^3[d_{xz} \rightarrow \pi^*]$
	IVb	221	4.52			$^1[d_{xz} \rightarrow \pi^*]$
trans-[Pt(PEt$_3$)$_2$Br$_2$]	I	435	2.30 sh	16		^{3}[LF]
(298 K)	II	333	3.00 sh	496		^{1}[LF]
	III	288	3.47 sh	5800	3.44 (+0.30)	π-LMCT
	IV	279	3.58	6300	3.62 (−0.36)	$^3[d_{yz} \rightarrow \pi^*]$
	V	252	3.96	4800	3.97 (−0.19)	$^1[d_{z^2} \rightarrow \pi^*]$
	VI	221	4.53 sh	14200		$^3[d_{xz} \rightarrow \pi^*]$
	VII	210	4.75 sh	21300		$^1[d_{xz} \rightarrow \pi^*]$
	VIII	200	5.00	58700	4.85 (−3.3), 4.95 (0), 5.10 (+2.6)	σ-LMCT
trans-[Pt(PEt$_3$)$_2$Br$_2$][d]	I	435	2.30	20		^{3}[LF]
(298 K)	II	330	3.03	455		^{1}[LF]
	III, IV	282	3.55	7780		π-LMCT/$^3[d_{yz} \rightarrow \pi^*]$
	V	257 sh	3.89	4830		$^1[d_{z^2} \rightarrow \pi^*]$
trans-[Pt(PEt$_3$)$_2$I$_2$]	I	334	2.99	2620	2.92 (+0.22)	π-LMCT
(298 K)	II	299	3.35	3370	3.30 (−0.30)	$^3[d_{yz} \rightarrow \pi^*]$
	III	283	3.53	6480	3.50 (−0.42)	$^1[d_{z^2} \rightarrow \pi^*]$
	IV	250	4.00 sh	12200	3.88 (+0.22)	$^1[d_{yz} \rightarrow \pi^*]$
	V	226	4.43	48800	4.31 (−1.7), 4.44 (0)	σ-LMCT
	VI	207	4.83	28600	4.62 (−1.4), 4.72 (0), 4.90 (~+1.2)	intraligand or d → p

[a] CH_3CN solution unless otherwise indicated. [b] $[\theta]_m = 3300\Delta A/MlH$. [c] Reference 4. [d] 7/4 methylcyclohexane/pentane solution.

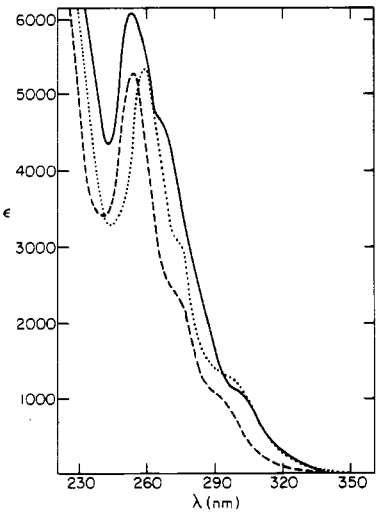

Figure 5. Electronic absorption spectra of *trans*-$[Pt(PEt_3)_2(H)Cl]$ (—), *trans*-$[Pt(PEt_3)_2(Me)Cl]$ (---), and *trans*-$[Pt(PEt_3)_2(Et)Cl]$ (···) in CH_3CN solution.

Band IV at 4.56 μm^{-1} in *cis*-$[Pt(PEt_3)_2Cl_2]$ and bands II and V in *cis*-$[Pt(PEt_3)_2Br_2]$ at 3.37 and 4.4 μm^{-1}, respectively, also have no counterpart in the spectrum of the dimethyl complex. These intense bands are attributed to LMCT transitions from the halide orbitals. Charge-transfer bands of the LMCT type have been characterized for $[PtCl_4]^{2-}$ and $[PtBr_4]^{2-}$ and lie at comparable energies to those observed here for the chloro and bromo complexes, respectively.[8,15] The lower energy band II in the dibromo complex and band IV in the dichloro complex are assigned to transitions from the halide orbitals of π symmetry, designated π-LMCT, while the higher energy band V in the dibromo complex is assigned to a transition from a halide orbital of σ symmetry and is designated σ-LMCT. The difference in absorptivity between the π-LMCT bands for the dichloro and dibromo complexes is likely due to the proximity to an intense MLCT transition in the former case.

The MLCT transitions in the dichloro and dibromo complexes follow the same pattern as for the dimethyl complex. The $^3[d_{z^2} \rightarrow \pi^*]$ transition at 3.81 μm^{-1} has a positive pseudo-*A* term clearly resolved in the MCD spectrum of *cis*-$[Pt(PEt_3)_2Cl_2]$. This term is analogous to the positive *A* term observed for the degenerate E_u component of the $^3[d_{z^2} \rightarrow \pi^*]$ transition in $[Pt(CN)_4]^{2-}$[4,14] and other Pt(II) and Ir(I) complexes[2,3,5] and thus indicates the closeness in energy of the component MLCT states of the $^3[d_{z^2} \rightarrow \pi^*]$ excitation.

***cis*-$[Pt(PEt_3)_2(Me)X]$ (X = Cl, Br).** The band patterns observed in the MCD and electronic absorption spectra of the *cis*-$[Pt(PEt_3)_2(Me)X]$ (X = Cl, Br) complexes are quite similar to those observed in the spectra of *cis*-$[Pt(PEt_3)_2Me_2]$. Analogous assignments are thus indicated (Table I). As in the case of *cis*-$[Pt(PEt_3)_2(Me)_2]$, band II of *cis*-$[Pt(PEt_3)_2(Me)Cl]$ is partially resolved into its component transitions in the 77 K spectrum (Table I).

***trans*-$[Pt(PEt_3)_2(X)(Y)]$ (X = Cl, Br; Y = H, Me, Et).** The electronic absorption and MCD spectra of all the trans complexes in the above series are remarkably similar to each other, and common MLCT assignments are thus indicated. A comparison of the electronic absorption spectra of the *trans*-$[Pt(PEt_3)_2(Y)Cl]$ (Y = H, Me, Et) complexes is shown in Figure 5. In these trans complexes, the d_{xz} orbital is directed toward the PEt_3 ligand and because of its π interactions is expected to be stabilized relative to d_{z^2} and d_{yz}. Thus MLCT transitions involving d_{xz} should lie at higher energy. The ordering of the d_{z^2} and d_{yz} orbitals cannot be as easily predicted. The MCD spectra of the *trans*-$[Pt(PEt_3)_2(X)(Y)]$ complexes show two positive *B* terms at lower energy followed by a pseudo-*A* term. This pattern implies that the $d_{z^2} \rightarrow \pi^*$ excitations are lower in energy than the $d_{yz} \rightarrow \pi^*$ excitations since a reversal of this energy ordering would lead to opposite signs for the MCD B terms because of the ΔW_{kj}^{-1} term in eq 1. Thus, the lowest energy bands which are clearly resolved in the MCD spectrum of each complex are assigned to the $^3[d_{z^2} \rightarrow \pi^*]$ and $^3[d_{yz} \rightarrow \pi^*]$ transitions in that order. The higher energy, overlapping transitions responsible for the positive pseudo-*A* term in each spectrum are assigned to $^1[d_{z^2} \rightarrow \pi^*]$ and $^1[d_{yz} \rightarrow \pi^*]$ with the former at slightly lower energy (negative ellipticity). Bands at higher energy still at ca. 4.4–4.5 and 4.6–4.7 μm^{-1} are assigned to the $^3[d_{xz} \rightarrow \pi^*]$ and $^1[d_{xz} \rightarrow \pi^*]$ transitions, respectively. Very intense bands are observed in each complex at 5.0–5.1 μm^{-1} which may be attributed to π-LMCT transitions or possibly d → p transitions from the d_{z^2} orbital to the $6p_z$ orbital of Pt. However, insufficient information is available to make firm assignments for these latter bands.

***trans*-$[Pt(PEt_3)_2X_2]$ (X = Cl, Br, I).** The band patterns observed in the MCD and absorption spectra of the *trans*-$[Pt(PEt_3)_2X_2]$ complexes are more complicated than those of the other trans complexes discussed above because of the presence of LF and LMCT transitions in these derivatives. Bands at 2.30 μm^{-1} (I, ϵ 16 M^{-1} cm^{-1}) and 3.00 μm^{-1} (II, ϵ 496 M^{-1} cm^{-1}) are apparent in the electronic absorption spectrum of *trans*-$[Pt(PEt_3)_2Br_2]$, and these are attributed to triplet and singlet LF transitions, respectively. Only the corresponding singlet LF transition at 3.28 μm^{-1} (I, ϵ 640 M^{-1} cm^{-1}) is resolved in the spectrum of the dichloro complex. The singlet LF transitions occur at nearly the same energy as the LF bands identified in the *cis*-dihalo complexes discussed above. Band III at 3.47 μm^{-1} and band VIII at 5.00 μm^{-1} in the dibromo complex are assigned as π-LMCT and σ-LMCT transitions, respectively. As expected, the corresponding LMCT bands for the diiodo complex are located at lower energy: 2.99 (π-LMCT) and 4.43 μm^{-1} (σ-LMCT). In each case the σ-LMCT band is very intense and exhibits a positive pseudo-*A* term in the MCD spectrum, analogous to the positive *A* terms previously observed for σ-LMCT transitions in several d^8 complexes of D_{4h} symmetry.[16] The diiodo complex exhibits another intense band at 4.83 μm^{-1} (VI) which may be an intraligand I^- transition or a d → p transition. Evidence to distinguish between these possibilities is not available. The remaining bands in the spectra of these complexes are attributed to MLCT transitions, and the specific assignments are set out in Table I.

Discussion

Each of the Pt(II) complexes examined in this study show well-defined MLCT bands in their electronic absorption and MCD spectra. Whether or not these transitions lie lowest in energy is a sensitive function of the nature of the X and Y ligands for a given complex. The positioning of the ligand-based acceptor orbital, largely derived from the PEt_3 phosphorus 3d orbitals, should be relatively invariant with changes in X and Y. However, because of the differing magnitude of the crystal field splitting induced by the X and Y ligands, the positioning of the metal 5d orbitals can vary significantly. For the ligands employed in this study the spectrochemical series follows the ordering H, Me, Et > PEt_3 > Cl > Br > I. When X = Y = Cl, Br, or I the empty metal d_σ orbital (d_{xy} in the cis complexes and $d_{x^2-y^2}$ in the trans complexes) falls below the ligand-based acceptor orbitals. In these complexes LF transitions lie lowest in energy. As expected, upon replacement of the halide ligands with H, Me, or Et ligands, the LF

(16) McCaffery, A. J.; Schatz, P. N.; Stephens, P. J. *J. Am. Chem. Soc.* **1968**, *90*, 5730.

Table II. MCD Band Positions (μm^{-1}) for *cis*-[Pt(PEt$_3$)$_2$(X)(Y)] Complexes

Me_2	MeCl	MeBr	Cl_2	Br_2	assignt	predicted MCD
3.21	3.45	3.44	3.79	3.72	$^3[d_{z^2} \rightarrow \pi^*]$	$+B$ or +pseudo-A term
3.66	4.00	3.95	4.16	4.10	$^1[d_{z^2} \rightarrow \pi^*]$, $^3[d_{xz}, d_{yz} \rightarrow \pi^*]$	+pseudo-A term
4.63	4.82		4.90	4.81	$^1[d_{xz}, d_{yz} \rightarrow \pi^*]$	+pseudo-A term

Table III. MCD Band Positions (μm^{-1}) for *trans*-[Pt(PEt$_3$)$_2$(X)(Y)] Complexes

HCl	HBr	MeCl	EtCl	MeBr	EtBr	Cl_2	Br_2	I_2	assignt	predicted MCD
3.24	3.22	3.32	3.26	3.33	3.27				$^3[d_{z^2} \rightarrow \pi^*]$	$+B$
3.52	3.47	3.61	3.55	3.58	3.57	3.65	3.62	3.30	$^3[d_{yz} \rightarrow \pi^*]$	$+B$
3.80	3.70	3.82	3.77	3.77	3.73	3.82	3.97	3.50	$^1[d_{z^2} \rightarrow \pi^*]$	$+B$
4.02	3.97	4.03	3.98	4.02	3.97	4.18		3.88	$^1[d_{yz} \rightarrow \pi^*]$	$-B$
4.48	4.48	4.37		4.35	4.48	4.46			$^3[d_{xz} \rightarrow \pi^*]$	$+B$
4.63	4.68			4.60[a] sh		4.76			$^1[d_{xz} \rightarrow \pi^*]$	$-B$

[a] Band in absorption spectrum.

transitions move to higher energy and the MLCT transitions lie at lower energy than the LF bands.

When X = Y = Cl, Br, or I, intense LMCT transitions associated with the halide ligands are also observed and occur among the MLCT transitions. These bands are easily identified because they are strongly halide dependent with relative energies Cl > Br > I. For *trans*-[Pt(PEt$_3$)$_2$I$_2$], the lowest energy band (I) at 2.99 μm^{-1} is assigned as the π-LMCT transition which obscures the lowest energy MLCT band, $^3[d_{z^2} \rightarrow \pi^*]$, and weaker LF transitions. As expected, the empty metal d orbital is destabilized, and the LMCT transitions blue shift when a halide ligand is replaced by the stronger σ donors H, Me, and Et.

The effect of varying the X and Y ligands on the MLCT bands for the various complexes can be seen in the data set out in Tables I–III. For the cis complexes the observed energy orderings for the $^3[d_{z^2} \rightarrow \pi^*]$ and $^1[d_{z^2} \rightarrow \pi^*]$ transitions are $Me_2 < MeX < X_2$ (X = Cl, Br). Since the position of an MLCT transition is a sensitive function of occupied metal orbital stability (metal oxidation state), this series indicates that, as the halide ligands are successively replaced by methyl ligands, the metal orbitals become less stable; i.e., the metal becomes less oxidized. This, of course, reflects a greater charge donation from the methyl ligands due to their higher σ-donor ability as compared to the halide ligands. A similar shift, though somewhat smaller, is noted for the $^1[d_{xz}, d_{yz} \rightarrow \pi^*]$ transition.[17]

The observed energy ordering $Et_2 < Me_2$ for the *cis*-[Pt(PEt$_3$)$_2$(R)$_2$] complexes implies that the metal ion is less oxidized in the former complex due to the greater σ-donor strength of the ethyl ligands. The latter is presumably due to the increased electron density on the ligating carbon of the ethyl ligand due to the inductive effect of the CH_3 substituent. In this regard, these results are consistent with Chen and Kochi's[18] electrochemical results in which they observed that *cis*-[Pt(PMe$_2$Ph)$_2$Et$_2$] is much easier to oxidize than is *cis*-[Pt(PMe$_2$Ph)$_2$Me$_2$] (0.72 vs. 0.40 V; vs. Ag/0.1 M $AgNO_3$).

In the trans complexes the energy ordering of the MLCT bands generally parallels the σ-donor strength of the ligands with $HX < EtX < MeX < X_2$ (X = Cl, Br), although the variation in band position is small.[17] In fact the spectra of the trans complexes where X = halide and Y = H, Me, or Et are remarkably similar (Figure 5). It is noteworthy that the MLCT transitions for the XEt complexes lie at lower energy than those of the XMe complexes (Table I) for the reasons discussed above, and furthermore, the orderings HX < MeX (X = Cl, Br) indicates that the metal ion is less oxidized in the hydride complexes as compared to the methyl derivatives. The relative insensitivity of the position of the $^3[d_{yz} \rightarrow \pi^*]$ and $^1[d_{yz} \rightarrow \pi^*]$ bands in all the complexes except for *trans*-[Pt(PEt$_3$)$_2$I$_2$] indicates that π donation from the chloride and bromide ligands to d_{yz} in the trans complexes is relatively small. The somewhat lower energies observed for the diiodo complex would be consistent with greater charge donation from iodide to the platinum as expected since I^- is a more strongly reducing ligand than either Br^- or Cl^-.

Table IV. Comparative MLCT Transition Energies (μm^{-1})

complex	$^1[d_{z^2} \rightarrow \pi^*]$	$^1[d_\pi \rightarrow \pi^*]$	$\Delta_{\pi-\sigma}$
$[Pt(CN)_4]^{2-}$ [a]	3.85	4.55	0.70
$[Pt(CNEt)_4]^{2+}$ [b]	3.93	4.83	0.90
cis-[Pt(PEt$_3$)$_2$(CH$_3$)$_2$]	3.66	4.63	0.97
cis-[Pt(PEt$_3$)$_2$(CH$_3$)Cl]	4.00	4.82	0.82
cis-[Pt(PEt$_3$)$_2$Cl$_2$]	4.16	4.90	0.74
cis-[Pt(PEt$_3$)$_2$Br$_2$]	4.10	4.81	0.71
trans-[Pt(PEt$_3$)$_2$(H)Cl]	3.80	4.63	0.83
trans-[Pt(PEt$_3$)$_2$(H)Br]	3.83	4.68	0.85
trans-[Pt(PEt$_3$)$_2$Cl$_2$]	3.82	4.76	0.94
trans-[Pt(PEt$_3$)$_2$Br$_2$]	3.96	4.75	0.79

[a] Reference 4. [b] Reference 5.

The π-acceptor ability of the PEt_3 ligand in the *cis*- and *trans*-[Pt(PEt$_3$)$_2$(X)(Y)] complexes can be compared qualitatively with CN^- and CNEt from the data collected in Table IV. The d_{z^2} orbital is weakly antibonding or nearly nonbonding in these complexes, while the d_π orbitals (d_{xz} and d_{yz} in a D_{4h} or a cis complex and d_{xz} in a trans complex) are stabilized due to π interactions with the π-accepting ligands. An increased π-acceptor ability of the ligand results in a greater energy difference, $\Delta_{\pi-\sigma}$, between corresponding MLCT bands originating from these two types of metal orbitals. The data in Table IV show that $\Delta_{\pi-\sigma}$ for the *cis*- and *trans*-[Pt(PEt$_3$)$_2$(X)(Y)] complexes is dependent upon X and Y but generally lies between that for $[Pt(CN)_4]^{2-}$ and $[Pt(CNEt)_4]^{2+}$. Thus, this study implies that PEt_3 is a better π acceptor than CN^- and is comparable to or slightly less than CNEt.

The observed solvent effect on the electronic absorption spectra of *trans*-[Pt(PEt$_3$)$_2$Cl$_2$] (Figure 6 and Table I) is interesting. Bands II and III change markedly when the solvent is changed from CH_3CN to the methylcyclohexane/pentane mixture. The former is weakly coordinating, presumably perpendicular to the plane of the molecule, and hence can alter the energies of the d orbitals. The orbitals most affected upon

(17) Comparison of MLCT band energies in related complexes includes a component reflecting differences in electron repulsions in the MLCT states. While these differences are presumed small, they could be large enough to account for the small differences observed between corresponding complexes.

(18) Chen, J. Y.; Kochi, J. K. *J. Am. Chem. Soc.* **1977**, *99*, 1450.

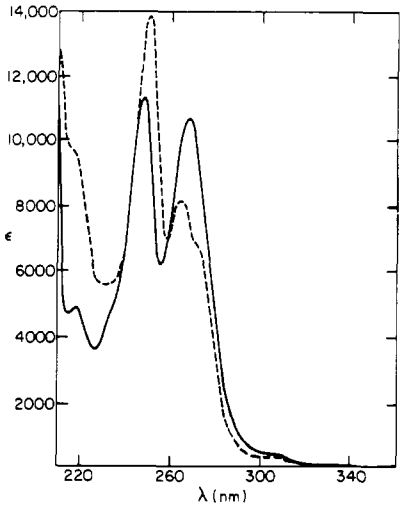

Figure 6. Electronic absorption spectrum of *trans*-$[Pt(PEt_3)_2Cl_2]$ in CH_3CN (—) and 7/4 methylcyclohexane/pentane (---) solution at 298 K.

coordination is d_{z^2} which should be destabilized in the solvated complex. Hence MLCT transitions which involve depopulation of this orbital will lie at lower energy in CH_3CN than in the noninteracting hydrocarbon solvents. Band II is a single peak (3.74 μm^{-1}) in CH_3CN solution but is resolved into two components in hydrocarbon solution (Figure 6 and Table I). The IIb peak at 3.80 μm^{-1} in hydrocarbon solution is attributed to the $^1[d_{z^2} \rightarrow \pi^*]$ transition from the MCD data, and indeed it does shift to lower energy (3.74 μm^{-1}) in CH_3CN solution. The $^3[d_{yz} \rightarrow \pi^*]$ transition seen as a shoulder (IIa) at 3.70 μm^{-1} in hydrocarbon solution apparently blue shifts to 3.74 μm^{-1} in CH_3CN solution, implying partial stabilization of the d_{yz} orbital via π interaction with the weakly π-accepting CH_3CN. The *trans*-$[Pt(PEt_3)_2Br_2]$ complex appears to show a similar solvent shift, but the effect is largely masked by the presence of the intense π-LMCT band in this spectral region (Table I). It is interesting that none of the other complexes examined in this work show such a solvent effect, but we can offer no explanation for this observation.

Finally, the results described herein are relevant to a recent photochemical study of related complexes. Costanzo et al.[19] recently reported that *cis*- and *trans*-$[Pt(PEt_3)_2(Ph)Cl]$ undergo photoinduced cis $\rightleftarrows$ trans isomerization in acetonitrile solution. Quantum yields were measured, and the observed wavelength effects were rationalized on the basis of the different excited states involved. The latter were deduced from an interpretation of the electronic absorption spectra of these derivatives in which the observed bands were attributed to LF and LMCT transitions. However, the electron absorption spectra of *cis*-$[Pt(PEt_3)_2(Ph)Cl]$ (λ 280 nm, ϵ 1600 M^{-1} cm^{-1}; λ 245 nm, ϵ 990 M^{-1} cm^{-1})[19] and *trans*-$[Pt(PEt_3)_2(Ph)Cl]$ (λ 290 nm, ϵ 1250 M^{-1} cm^{-1}; λ 255 nm, ϵ 5300 M^{-1} cm^{-1})[19] are virtually identical with those of the *cis*- and *trans*-$[Pt(PEt_3)_2(Me)Cl]$ complexes studied herein (Table I) for which the observed bands have been assigned as MLCT transitions. Common MLCT assignments for the observed bands in the *cis*- and *trans*-$[Pt(PEt_3)_2(Ph)Cl]$ complexes are thus indicated. The excited-state arguments given by Costanzo et al.[19] to rationalize their photochemical results are therefore inappropriate, and the observed photochemistry of the *cis*- and *trans*-$[Pt(PEt_3)_2(Ph)Cl]$ complexes should be reassessed in view of the correct MLCT assignments.

Acknowledgment. This work was supported by the National Science Foundation. G.L.G. gratefully acknowledges the Camille and Henry Dreyfus Foundation for a Teacher-Scholar Award and the Alfred P. Sloan Foundation for a research fellowship.

Registry No. *cis*-$[Pt(PEt_3)_2Me_2]$, 22289-34-5; *cis*-$[Pt(PEt_3)_2Et_2]$, 75847-39-1; *cis*-$[Pt(PEt_3)_2Cl_2]$, 15692-07-6; *cis*-$[Pt(PEt_3)_2Br_2]$, 15636-78-9; *cis*-$[Pt(PEt_3)_2(Me)Cl]$, 22289-46-9; *cis*-$[Pt(PEt_3)_2(Me)Br]$, 22289-47-0; *trans*-$[Pt(PEt_3)_2(H)Cl]$, 16842-17-4; *trans*-$[Pt(PEt_3)_2(Me)Cl]$, 13964-96-0; *trans*-$[Pt(PEt_3)_2(Et)Cl]$, 54657-72-6; *trans*-$[Pt(PEt_3)_2(H)Br]$, 18660-33-8; *trans*-$[Pt(PEt_3)_2(Me)Br]$, 15691-67-5; *trans*-$[Pt(PEt_3)_2(Et)Br]$, 75847-40-4; *trans*-$[Pt(PEt_3)_2Cl_2]$, 13965-02-1; *trans*-$[Pt(PEt_3)_2Br_2]$, 13985-90-5; *trans*-$[Pt(PEt_3)_2I_2]$, 15636-79-0.

(19) Costanzo, L. L.; Giuffrida, S.; Romeo, R. *Inorg. Chim. Acta* **1980**, *38*, 31.

Contribution from the Department of Chemistry, University of Leuven, 3030 Heverlee, Belgium

On the Ligand Field Spectra of Square-Planar Platinum(II) and Palladium(II) Complexes

L. G. VANQUICKENBORNE* and A. CEULEMANS

Received March 26, 1980

The electronic structure of square-planar complexes is apparently characterized by an anomalously low-lying a_{1g} (d_{z^2}) orbital. An attempt is made to describe the situation by using a semiempirical correction parameter σ_{sd}. A number of ligand field spectra of Pt(II) and Pd(II) complexes are analyzed and (re)interpreted on the basis of this procedure. The nature of the σ_{sd} parameter is discussed in terms of second-order perturbation theory.

Introduction

From the point of view of ligand field theory, the electronic structure of square-planar coordination compounds is characterized by a number of unusual features.[1-4] Most of the observed anomalies appear to be related to the energy and the nature of the a_{1g} (d_{z^2}) orbital. The fact that this orbital is apparently situated at much lower energy than can be expected from ligand field considerations is thought to be due to an (n + 1)s–nd mixing phenomenon.[5-11]

(1) D. S. Martin, *Inorg. Chim. Acta, Rev.*, **5**, 107 (1971).
(2) J. Chatt, G. A. Gamlen, and L. E. Orgel, *J. Chem. Soc.*, 486 (1958).
(3) T. J. Peters, R. F. Krŏning, and D. S. Martin, *Inorg. Chem.*, **17**, 2302 (1978).
(4) M. A. Hitchman and P. J. Cassidy, *Inorg. Chem.*, **18**, 1745 (1979).
(5) H. Basch and H. B. Gray, *Inorg. Chem.*, **6**, 365 (1967).
(6) F. A. Cotton and C. B. Harris, *Inorg. Chem.*, **6**, 369 (1967).

0020-1669/81/1320-0796$01.00/0